

Mapping the $G\beta\gamma$ -binding Sites in GIRK1 and GIRK2 Subunits of the G Protein-activated K^+ Channel*

Received for publication, April 30, 2003, and in revised form, May 8, 2003
Published, JBC Papers in Press, May 12, 2003, DOI 10.1074/jbc.M304518200

Tatiana Ivanina, Ida Rishal, Dalia Varon, Carmen Müllner‡§, Bibiane Frohnwieser-Steinecke‡, Wolfgang Schreibmayer‡, Carmen W. Dessauer¶, and Nathan Dascal||

From the Department of Physiology and Pharmacology, Sackler School of Medicine, Tel Aviv University, Ramat Aviv 69978, Israel, ‡Institute for Medical Physics and Biophysics, Graz University, A8010 Graz, Austria, and the ¶Department of Integrative Biology and Pharmacology, Houston Medical School, University of Texas, Houston, Texas 77030

G protein-activated K^+ channels (Kir3 or GIRK) are activated by direct binding of $G\beta\gamma$. The binding sites of $G\beta\gamma$ in the ubiquitous GIRK1 (Kir3.1) subunit have not been unequivocally charted, and in the neuronal GIRK2 (Kir3.2) subunit the binding of $G\beta\gamma$ has not been studied. We verified and extended the map of $G\beta\gamma$ -binding sites in GIRK1 by using two approaches: direct binding of $G\beta\gamma$ to fragments of GIRK subunits (pull down), and competition of these fragments with the $G\alpha_{i1}$ subunit for binding to $G\beta\gamma$. We also mapped the $G\beta\gamma$ -binding sites in GIRK2. In both subunits, the N terminus binds $G\beta\gamma$. In the C terminus, the $G\beta\gamma$ -binding sites in the two subunits are not identical; GIRK1, but not GIRK2, has a previously unrecognized $G\beta\gamma$ -interacting segments in the first half of the C terminus. The main C-terminal $G\beta\gamma$ -binding segment found in both subunits is located approximately between amino acids 320 and 409 (by GIRK1 count). Mutation of C-terminal leucines 262 or 333 in GIRK1, recognized previously as crucial for $G\beta\gamma$ regulation of the channel, and of the corresponding leucines 273 and 344 in GIRK2 dramatically altered the properties of K^+ currents via GIRK1/GIRK2 channels expressed in *Xenopus* oocytes but did not appreciably reduce the binding of $G\beta\gamma$ to the corresponding fusion proteins, indicating that these residues are mainly important for the regulation of $G\beta\gamma$ -induced changes in channel gating rather than $G\beta\gamma$ binding.

G protein-activated K^+ channels (Kir3 or GIRK)¹ mediate postsynaptic inhibitory effects of many transmitters in heart and brain via G protein-coupled receptors such as opioid, α -adrenergic, muscarinic cholinergic, γ -aminobutyric acid-B, cannabinoid, etc. The mediator of neurotransmitter action is $G\beta\gamma$ derived from

heterotrimeric G proteins of the $G_{i/o}$ class. $G\beta\gamma$ acts by directly binding to the channel molecule. Historically, GIRK was the first identified $G\beta\gamma$ effector (reviewed in Refs. 1–3).

Four GIRK subunits are known in mammals, GIRK1 to GIRK4. A functional channel is composed of four identical subunits (homotetramer) or different subunits (heterotetramer). Heterotetramers appear to compose the majority of functional GIRK channels in the body. GIRK1/2, GIRK1/3, and GIRK2/3 channels are abundant in the brain, and GIRK1/4 is predominant in the heart (4–9). Heterotetrameric GIRK1/2 and GIRK1/4 channels contain a pair of each subunits, giving a GIRK1₂GIRKx₂ stoichiometry. As in all inward rectifier K channels of the Kir family, each subunit consists of a core transmembrane domain flanked by cytoplasmic N and C termini (reviewed in Ref. 10). The structure of the core domain, which contains two membrane-spanning α -helices M1 and M2 and a reentrant helix-P-loop, follows the universal K^+ channel pattern (11). The three-dimensional structure of a major section of the cytoplasmic domain of GIRK1 has been resolved recently (12). The crystal structure shows that four cytoplasmic domains, without the transmembrane core domain, form a tetramer that folds to encircle a 60-Å-long cytoplasmic water-filled channel, presumably a direct continuation of the transmembrane channel; the external walls of this structure are exposed to the cytoplasm.

Direct binding of $G\beta\gamma$ to GIRK has been studied only in GIRK1 and GIRK4; in both, $G\beta\gamma$ binds to the cytoplasmic N and C termini (6, 13–17). The exact location of $G\beta\gamma$ -binding sites in GIRK1 and GIRK4, and their functional impact, are not unequivocal. Up to three separate $G\beta\gamma$ -binding segments in each subunit have been reported; not all are identical in GIRK1 and GIRK4. We designated the various proposed $G\beta\gamma$ -binding segments as sites 1–4 for simplicity (see Fig. 1). The N-terminal $G\beta\gamma$ -binding site 1, and a mid-C-terminal site 3, amino acids (a.a.) ~318–374 (numbering by GIRK1), were identified by direct binding (pull down) experiments between $G\beta\gamma$ and GST-fused GIRK fragments, and are present both in GIRK1 and GIRK4 subunits (13, 15, 17–19). Peptide competition experiments tested the ability of 20-mer peptides, corresponding to cytosolic segments of GIRK1 and GIRK4, to inhibit the binding of $G\beta\gamma$ to purified GIRK1/4 protein. These experiments, in conjunction with mutagenesis, suggested a high affinity site 2 in the proximal part of the C terminus of GIRK4 (a.a. ~209–245 in GIRK4). Corresponding peptides from GIRK1 produced little or no inhibition of $G\beta\gamma$ -GIRK1/4 binding, implying that GIRK1 lacks this binding site (20). Later binding studies with GST fusion proteins of GIRK4 (19) did not assign a major role for site 2 in $G\beta\gamma$ -GIRK4 binding and implicated the region between a.a. 253 and 348 in GIRK4 as a

* This work was supported by grants from the United States-Israel Binational Science Foundation (to N. D. and C. D.), National Institutes of Health Grants GM60419 (to C. D.) and GM68493 (to N. D.), Austrian Research Foundation Grant SFB007/F708 (to W. S.), and Austrian Ministry of Science Grant UGP4 (to W. S.). The costs of publication of this article were defrayed in part by the payment of page charges. This article must therefore be hereby marked "advertisement" in accordance with 18 U.S.C. Section 1734 solely to indicate this fact.

§ Present address: Institute of Pharmacology and Toxicology, Innsbruck University, 6020 Innsbruck, Austria.

|| To whom correspondence should be addressed: Dept. of Physiology and Pharmacology, Sackler School of Medicine, Tel Aviv University, Tel Aviv 69978, Israel. Tel.: 972-3-6405743; Fax: 972-3-6409113; E-mail: dascaln@post.tau.ac.il.

¹ The abbreviations used are: GIRK, G protein-activated K^+ channel; a.a., amino acid; GST, glutathione *S*-transferase; WT, wild-type; ACh, acetylcholine; CHAPS, 3-[(3-cholamidopropyl)dimethylammonio]-1-propanesulfonic acid; GTP γ S, guanosine 5'-3-*O*-(thio)triphosphate.

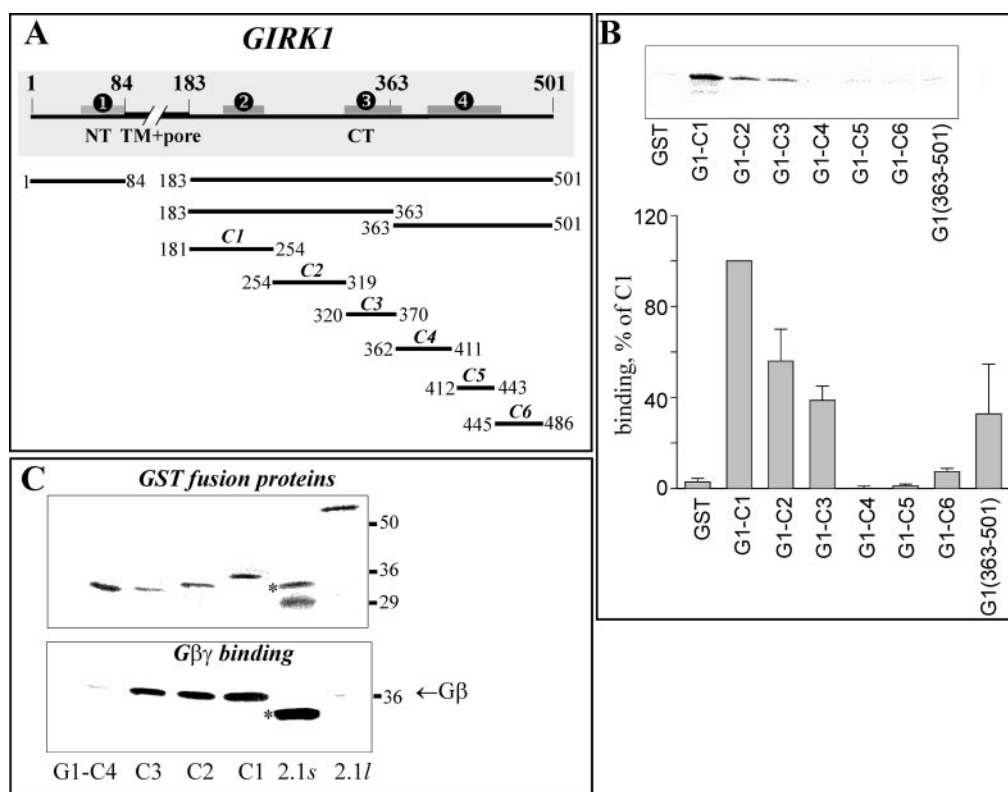


FIG. 1. Direct interaction of GST fusion proteins from the C terminus of GIRK1 with $G\beta\gamma$. *A*, schematic linear presentation of the GIRK1 subunit (*thick bar* at the top; the membrane-spanning region is shown *with gap*) and the GST fusion proteins used in pull-down experiments (the *shorter bars*, with numbers indicating the first and the last a.a. of the fragment fused to GST) is shown. The previously identified or proposed $G\beta\gamma$ -binding sites are shown in *gray*, numbered 1 to 4. Site 2 has been proposed to exist only in GIRK4 but not in GIRK1 (20). *B*, binding of *in vitro* synthesized $G\beta\gamma$ to GST fusion proteins monitored by direct reading of radioactive signals with PhosphorImager. *Upper panel* shows an autoradiogram from a representative experiment. The *lower panel* is a summary of four experiments (GST, G1-C1, G1-C2, and G1-C3 were present in all experiments, the other fusion proteins in three experiments). In each experiment, the signal measured by the PhosphorImager was corrected for the amount of fusion protein in each band. All signals were normalized to that of $G\beta\gamma$ bound to G1-C1. *C*, binding of purified recombinant $G\beta\gamma$ to GIRK1 fusion proteins as monitored by Western blot analysis. Coomassie Blue staining of the GST fusion proteins is shown in the *upper panel*. The *lower panel* is a Western blot using the anti- $G\beta$ antibody and is representative of three independent experiments. For unknown reasons, the antibody non-specifically labeled the 2.1s protein (denoted by the *asterisk*). Note that there was no labeling at the 36-kDa level (the size of $G\beta$) in the ECL signal of 2.1s.

minimal C-terminal $G\beta\gamma$ -binding segment. Finally, some pull-down experiments suggested the presence of a unique distal site 4 in GIRK1 (a.a. 390–462) but not in GIRK4 (17). However, peptides from this region did not affect the binding of $G\beta\gamma$ to purified GIRK1/4 (20). Thus, the $G\beta\gamma$ -binding surface of GIRK1 remains to be better delineated.

A unique functional role has been assigned to site 3 as a low affinity site underlying agonist-induced activation (18). Mutation of Leu³³³ in site 3 of GIRK1 and the corresponding Leu³³⁹ in GIRK4 eliminate G protein-coupled receptor-induced activation but leave the $G\beta\gamma$ -dependent basal activity largely intact, implying that the latter may be determined by a distinct site (18). Recent studies by He *et al.* (19) point to a crucial role and a joint participation of specific residues in the N terminus and in the proximal C terminus (His⁵⁷ and Leu²⁶² in GIRK1 and His⁶⁴ and Leu²⁶⁸ in GIRK4) in the control of all $G\beta\gamma$ -dependent activity, basal and agonist-evoked, in GIRK1/4. Mutation of Leu²⁶⁸ has been reported to reduce the binding of $G\beta\gamma$ to a GST fusion protein encompassing a.a. 253–348 of GIRK4, suggesting the importance of this residue in the interaction of GIRK4 with $G\beta\gamma$ (19). However, in GIRK1, Leu²⁶² lies well outside any previously identified $G\beta\gamma$ -binding sites, again calling for a better mapping of $G\beta\gamma$ -binding surfaces in GIRK1.

This study addresses the mechanisms associated with the binding of $G\beta\gamma$ to the C-terminal region of two GIRK subunits, the ubiquitous GIRK1 and a highly important neuronal GIRK2 subunit, and the relation between the roles of several crucial

amino acids in $G\beta\gamma$ binding and channel gating. We also address the correspondence between the $G\beta\gamma$ -binding sites identified by standard biochemical methods and the recently revealed crystal structure of the cytoplasmic domain of GIRK1. Surprisingly, the standard pull-down approach suggested the presence of a very large $G\beta\gamma$ -binding surface in GIRK1, which included sites 1–3, whereas in GIRK2 $G\beta\gamma$ bound only to fragments corresponding to sites 1 and 3 defined above. An alternative indirect approach, in which GST-fused fragments of GIRK1 were assayed for their ability to prevent the interaction between $G\alpha_{i1}$ and $G\beta\gamma$, suggested a prominent C-terminal $G\beta\gamma$ -interacting segment between a.a. 336 and 409, that is most of site 3 and part of site 4. Mutation of the crucial C-terminal leucines 262 and 333 in GIRK1 and the corresponding leucines 273 and 344 in GIRK2 dramatically altered the function of heterotetrameric GIRK1/2 channels. However, these mutations did not significantly reduce $G\beta\gamma$ binding to relevant GST fusion fragments, suggesting that their involvement in the interaction with $G\beta\gamma$ is mainly relevant to changes in GIRK gating rather than $G\beta\gamma$ binding.

MATERIALS AND METHODS

cDNA Constructs and RNA—GST-GIRK1 and GST-GIRK2 fusion constructs were created using PCR. DNA fragments encoding the indicated amino acid residues (Figs. 1A, 2A, and 3D) from rat GIRK1, mouse GIRK2, and mouse Kir2.1 were cloned into the vector pGEX-cs or pGEX-4T-1 (21) using the restriction enzymes *Bam*HI and *Nco*I, *Bam*HI and *Xho*I, or *Eco*RI and *Not*I. All DNA constructs were verified

by nucleotide sequencing. We found a variation, possibly polymorphic, in the reported mouse GIRK2 cDNA (22); a.a. 344, reported to be methionine, was found to be leucine. RNA for protein expression in *Xenopus* oocytes and in rabbit reticulocyte lysate was synthesized from cDNAs of m2R, GIRK subunits, G β_1 and G γ_2 as described previously (23, 24).

Xenopus Oocytes Preparation and Electrophysiology—*Xenopus* oocytes were prepared, injected with RNA, and incubated in ND-96 solution (96 mM NaCl, 2 mM KCl, 1 mM CaCl₂, 1 mM MgCl₂, 5 mM Hepes/NaOH (pH 7.6)) supplemented with gentamycin (50 μ g/ml) and sodium pyruvate (2.5 mM). Data acquisition and analysis were done using the Axotape and the pCLAMP software (Axon Instruments Inc., Foster City, CA). All experiments were done at 20–22 °C. Whole-cell GIRK currents were measured using a two-electrode voltage clamp. Oocytes were voltage-clamped at –80 mV in the ND-96 solution, and GIRK currents were measured in a high K⁺ solution containing 96 mM KCl, 2 mM NaCl, 1 mM CaCl₂, 1 mM MgCl₂, 5 mM Hepes (pH 7.5), as described (25, 26).

Purification of Recombinant Proteins—Myristoylated G α_{i1} and G $\beta\gamma$ were purified from *Escherichia coli* and *Sf9* cells as described previously (27, 28). GST-GIRK fusion proteins were expressed in BL21(DE3) or BL21(RIL) cells and purified using glutathione affinity resin, as described (29). Protein was eluted from the glutathione affinity resin with 20 mM Hepes, 1 mM EDTA, 2 mM dithiothreitol, 5 mM KCl, and 10 or 15 mM glutathione. In some cases, protein was then concentrated and dialyzed overnight in elution buffer lacking glutathione.

Inhibition of G $\beta\gamma$ -mediated ADP-ribosylation—The capacity of G $\beta\gamma$ to support the ADP-ribosylation of recombinant myristoylated G α_{i1} was assessed as described, with minor modifications (30). The final dimyristoylphosphatidylcholine lipid concentration was increased to 1 mM, and purified G α_{i1} (20 pmol/assay) was used as substrate. G α_{i1} , G $\beta\gamma$ (0.3 pmol/assay), and GST-GIRK1 fusion proteins were added on ice in a final volume of 25 μ l. The reaction was started with 15 μ l of pertussis toxin mix and incubated for 20 min at 30 °C. The reaction was stopped, and the amount of [³²P]NAD incorporated was assessed by filter binding using 6% ice-cold trichloroacetic acid.

Interaction between GST Fusion Proteins and G $\beta\gamma$ —With *in vivo* synthesized G $\beta\gamma$, the procedures were essentially as described (29), with minor modifications. In brief, [³⁵S]Met-labeled G β_1 and G γ_2 were translated on the template of *in vitro* synthesized RNAs using a rabbit reticulocyte translation kit (Promega). Purified GST fusion proteins (5–10 μ g) were incubated with 5 μ l of the lysate (in the case of *in vitro* synthesized G $\beta\gamma$) containing the ³⁵S-labeled proteins in 300 μ l of phosphate-buffered saline or high K⁺ buffer (in mM: 150 KCl, 50 Tris, 5 MgCl₂, 1 EDTA (pH 7.0)) with the addition of 0.5% CHAPS, for 1 h at room temperature, with gentle rocking. Then 30 μ l of glutathione-Sepharose beads (Amersham Biosciences) were added, and the mixture was incubated for 30 min at 4 °C and washed three times in 1 ml of the same buffer, first time with 0.5% CHAPS and in the following with 0.1% CHAPS. Following washing, GST fusion proteins were eluted with 30 μ l of 15 mM reduced glutathione in elution buffer (120 mM NaCl, 100 mM Tris-HCl (pH 8)) and analyzed on 12% SDS-polyacrylamide gels. The labeled products were identified and quantified by autoradiography using a PhosphorImager (Amersham Biosciences) as described (31). In the summary shown in Fig. 1B, the radioactive signals obtained by PhosphorImager were additionally corrected for the differences in the amount of fusion proteins in each band in the following way. The dried gels, with proteins stained by Coomassie Blue, were scanned to a bitmap file, and the relative amount of each protein in a band was measured in arbitrary OD units using TINA software (Raytest, Straubenhardt, Germany) and then normalized to the amount of G1-C1 fusion protein (see Fig. 1A) in the same experiment. The differences between the amounts of the various GST fusion proteins estimated by this method never exceeded 2-fold.

With purified G $\beta_1\gamma_2$, the reaction contained 5 μ g of GST fusion protein and 1 μ l of 20 μ M purified G $\beta\gamma$, in a final volume of 100 μ l of phosphate-buffered saline containing 1 mM EDTA, 1 mM dithiothreitol, and Lubrol at 0.01% (32) or 0.1% (19). Similar results were obtained at both concentrations of Lubrol. The mixture was incubated for 30 min at 4 °C, and then glutathione-Sepharose beads were added, and the reaction proceeded as above for *in vitro* synthesized G $\beta\gamma$. The proteins were transferred from the polyacrylamide gels to nitrocellulose membranes for Western blotting with the common G β antibody (Calbiochem) at 1:750 dilution. The proteins were visualized using the SuperSignal Substrate ECL kit (Pierce).

Confocal Imaging of GIRK in Plasma Membrane—The level of GIRK1 protein in plasma membrane was measured as described (23, 33). Briefly, large oocyte membrane patches, free of any visible cytosolic

contaminants or pigment granules, were attached to coverslips, fixed, stained by a specific GIRK1 antibody (Alomone Labs, Jerusalem, Israel), and visualized using a Cy3-conjugated rabbit IgG (Jackson ImmunoResearch Laboratories) using the Zeiss LSM 410 confocal microscope. Intensity of labeling (OD units) was measured with TINA software.

Data Presentation and Statistics—Data are presented as mean \pm S.E. Comparison between two groups of treatment was done using the two-tailed Student's *t* test. Comparison between several groups of data has been performed using one-way analysis of variance followed by Dunnett's test.

RESULTS

Direct Binding of G $\beta\gamma$ to GST-fused Fragments of GIRK1 and GIRK2—We have probed G $\beta\gamma$ binding to different parts of GIRK1 by a standard pull-down approach, widely used in previous studies. A series of GST fusion proteins of various length, covering the cytoplasmic N- and C-terminal portions of GIRK1, has been prepared (Fig. 1A). The C terminus was arbitrarily subdivided into 6 fragments with little or no overlap; in addition, fusion proteins covering a.a. 183–363 and 363–501 (G1-(183–363) and G1-(362–501), respectively) and the whole C terminus (G1-(183–501)) were prepared. We measured the binding of [³⁵S]methionine-labeled G $\beta_1\gamma_2$, synthesized *in vitro* in rabbit reticulocyte lysate, to GST fusion proteins immobilized of glutathione-agarose affinity beads. The functional activity of *in vitro* synthesized G $\beta\gamma$ has been verified by its binding to a GST-fused G α_{i3} in the presence of GDP but not GTP γ S (24). *In vitro* synthesized, metabolically labeled G $\beta\gamma$ has been successfully used in the past to identify G $\beta\gamma$ -binding sites of voltage-gated Ca²⁺ channels (34, 35). It gives the advantage of a highly sensitive and accurate quantitation of bound protein, because the radioactive signal from labeled G $\beta\gamma$ is measured from dried gels by PhosphorImager directly, in an almost unlimited linear range, and with high precision. In comparison, in Western blotting, several additional intermediate steps are involved (transfer of protein to membranes, binding of secondary antibody, and chemiluminescent reaction) that reduce the accuracy of measurement.

In the initial experiments, we verified that, as reported previously (13, 15, 17), the whole-length N terminus (G1-(1–84)) and C terminus (G1-(183–501)) of GIRK1 and G1-(183–363) bind G $\beta\gamma$ (data not shown; see also Fig. 6A). Shorter fragments of the C terminus were explored in more detail. G1-C1, G1-C2, and G1-C3 reproducibly bound G $\beta\gamma$ (Fig. 1B). For comparison, we constructed a fusion protein 2.1s that presents a fragment from a homologous but G $\beta\gamma$ -insensitive inwardly rectifying K⁺ channel, Kir2.1, exactly corresponding to G1-C3 of GIRK1. This protein did not bind G $\beta\gamma$ (e.g. Fig. 6A). The lower panel of Fig. 1B summarizes the results of pull-down experiments, showing that G1-C2 and G1-C3 bound G $\beta\gamma$ to a similar extent, whereas G1-C1 bound the best (Fig. 1B). G1-(363–501), which covers all of the previously proposed (17) site 4 (a.a. 390–462), showed rather low G $\beta\gamma$ binding, which was also highly variable (data not shown). The latter suggests poor folding of this fusion protein (see also Ref. 17). Poor binding of G $\beta\gamma$ to a corresponding fragment of GIRK1-(357–501) was also reported by Kunkel and Peralta (15). None of the subdivisions of this fragment (G1-C4 through G1-C6) bound G $\beta\gamma$ (Fig. 1B).

G1-C1 and G1-C2 have not been designated previously as G $\beta\gamma$ -binding sites in GIRK1. To make sure that the binding to G1-C1 or G1-C2 is not due to some contamination present in the reticulocyte lysate, we tested the binding of highly purified recombinant G $\beta_1\gamma_2$, instead of *in vitro* synthesized G $\beta\gamma$, to the same fusion proteins; the bound G $\beta\gamma$ was visualized using Western blot methodology. As shown in Fig. 1C, the results were essentially the same as with *in vitro* synthesized G $\beta\gamma$. Whereas quantitative assessment in this case was less accurate, G1-C1, G1-C2, and G1-C3 clearly bound G $\beta\gamma$. Neither

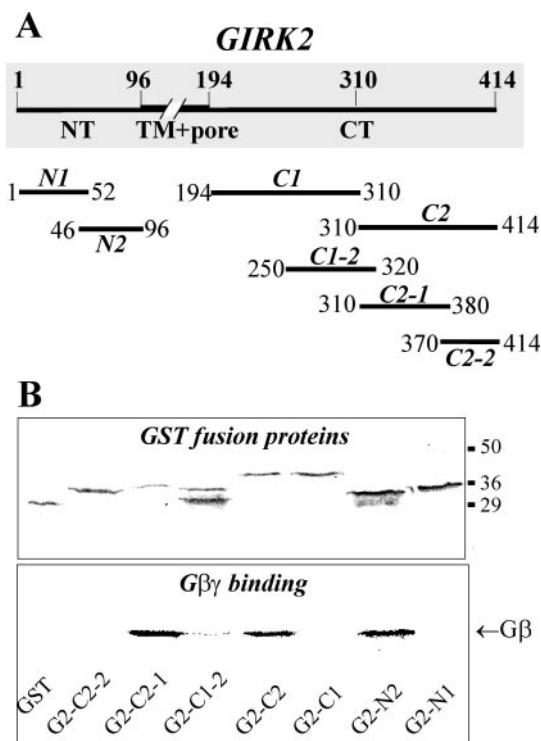


FIG. 2. Direct interaction of GST fusion proteins from GIRK2 with G $\beta\gamma$. *A*, schematic linear presentation of the GIRK2 subunit, and the GST fusion proteins used in pull-down experiments. *B*, binding of *in vitro* synthesized G $\beta\gamma$ to GST fusion proteins monitored by direct reading of radioactive signals with PhosphorImager. *Upper panel* shows Coomassie Blue staining of the GST fusion proteins; the *lower panel* shows the PhosphorImager autoradiogram. Representative of three separate experiments is shown. Note the strong G β signal in G2-C2-1, despite a relatively low amount of the loaded fusion protein.

G1-C4 nor the Kir2.1 fragment 2.1s bound any G $\beta\gamma$, but a weak binding to whole-length C terminus of Kir2.1 (2.1l) was sometimes observed.

We have similarly mapped the cytoplasmic parts of GIRK2, using *in vitro* synthesized G $\beta\gamma$ (Fig. 2), with GST fusion proteins that covered all of the N- and C-terminal cytoplasmic parts of GIRK2 (Fig. 2A). Fig. 2B shows that in the N terminus the distal but not the proximal half bound G $\beta\gamma$. In the C terminus, binding was observed only in the distal half (G2-C2), and within this segment, only the proximal part (G2-C2-1) bound G $\beta\gamma$ (this fragment corresponds to the end of G1-C2 and all of G1-C3 of GIRK1; see Fig. 7A). Thus, no G $\beta\gamma$ binding is found in the C terminus of GIRK2 at segments corresponding to the hypothetical sites 2 and 4 or to G1-C1 fragment of GIRK1. The fragment G2-C2-1, identified as sufficient for G $\beta\gamma$ binding, overlaps site 3.

Mapping G $\beta\gamma$ Binding Segments of C Terminus of GIRK1 by Competition with G α_{i1} ²—To obtain an independent measure of binding of G $\beta\gamma$ to segments of the C terminus of GIRK1, we chose to assay the competition between G α and C-terminal GST fusion proteins for the binding to G $\beta\gamma$. Such competition is reasonable, because at least some of the residues of G β that interact with GIRK are located at the G α -binding surface of G β (36). Our assay is based on the fact that ADP-ribosylation of G α_1 -GDP, catalyzed by pertussis toxin, is possible only in the heterotrimeric form of the G protein (37). If a GST fusion protein interacts with G $\beta\gamma$ and (sterically or allosterically) reduces the binding of G $\beta\gamma$ to G α , the pertussis toxin-catalyzed

incorporation of NAD into G α will be reduced. In these experiments, we used purified recombinant G $\beta_{1\gamma_2}$ and G α_{i1} ; we have verified that the latter does not bind to full-length C terminus of GIRK1 or any one of the fusion proteins G1-C1 through G1-C6.³ Therefore, only binding of the fusion proteins to G $\beta\gamma$ could interfere with ADP-ribosylation.

Fig. 3 (A–C) shows the results of three independent experiments with an extensive array of GST fusion proteins. The array of fusion proteins used and the results are summarized in Fig. 3D, where (+) indicates the ability of a given GST fusion protein to inhibit ADP-ribosylation of G α_{i1} -GDP. In this assay, the full-length C terminus of GIRK1 (G1-(183–501)) blocks G $\beta\gamma$ interactions with the G α subunit in a dose-dependent manner (Fig. 3A). Of all the GST fusion proteins tested, only those containing amino acids 336–409 were able to counteract ADP-ribosylation. G1-(336–409) was the shortest effective fusion protein. Neither G1-(183–363) that encloses G1-C1, G1-C2, and most of G1-C3 nor G1-(318–390) that covers all of the G1-C3 was effective in this assay. From the comparison of G1-(318–390) or G1-(336–390) with G1-(336–409), it is clear that the segment 390–409 was necessary for the prevention of ADP-ribosylation. However, it was insufficient, because neither G1-(360–454) nor G1-(380–454) was effective. A similar comparison between G1-(336–454) and G1-(360–454) indicates that the same is true for the segment 336–360; it is necessary but insufficient. In summary, these experiments indicate that a G $\beta\gamma$ -interacting surface, which is able to interfere with the binding of G $\beta\gamma$ to G α , is located in the region of C terminus of GIRK1 that extends at least between amino acids 336 and 409, roughly corresponding to previously identified sites 3 and 4.

Taken together, the results so far suggest that a C-terminal segment roughly corresponding to a.a 320–409 (GIRK1 count), and a similar segment in GIRK2, are prominent G $\beta\gamma$ -binding segments in both subunits. We have therefore focused on this segment for further analysis.

The Crucial C-terminal Leucines: Role in G $\beta\gamma$ Binding or Gating?—Leu³³³ and the corresponding Leu³³⁹ in GIRK4 are crucial for agonist-evoked responses in heterotetrameric GIRK1/4 (18). This residue is conserved in all GIRK channels but is replaced by Glu in the G $\beta\gamma$ -insensitive Kir2.1. The role of the corresponding Leu³⁴⁴ in GIRK2 has not been examined. Because this residue is located within or at least very close to the G $\beta\gamma$ -binding segments identified in our biochemical assays both in GIRK1 and GIRK2, we attempted to evaluate the role of this residue in G $\beta\gamma$ binding and in the gating of the heterotetrameric GIRK1/2 channels. Leu³³³ in GIRK1 and Leu³⁴⁴ in GIRK2 were mutated to Glu, as it has been done in GIRK1 and GIRK4 (18). In addition, in both subunits, we have mutated two other residues that have been proposed as crucial for interaction with G $\beta\gamma$ and both for basal and agonist-evoked activity in GIRK1 and GIRK4 (19). The N-terminal His⁵⁷ in GIRK1 and the homologous His⁶⁹ in GIRK2 were mutated to Phe, and the C-terminal Leu²⁶² in GIRK1 and Leu²⁷³ in GIRK2 were mutated to Ile.

Heterotetrameric GIRK1/2 channels containing the mutated residues were expressed in *Xenopus* oocytes (0.2 ng of RNA/oocyte), along with muscarinic m2 receptors, and basal and acetylcholine (ACh)-evoked currents were measured in high-K⁺ extracellular solution, using the two-electrode voltage clamp method (Fig. 4A). Basal GIRK current (I_{basal}) was revealed as a large inward K⁺ current developing upon the shift from a normal physiological solution with 96 mM Na⁺ and 2 mM K⁺ to a high K⁺ solution with 96 mM K⁺ and 2 mM Na⁺. I_{basal} showed a typical inactivation within 6–7 min, probably due to

² These experiments were performed in the laboratory of A. G. Gilman.

³ T. Ivanina, D. Varon, and N. Dascal, unpublished observations.

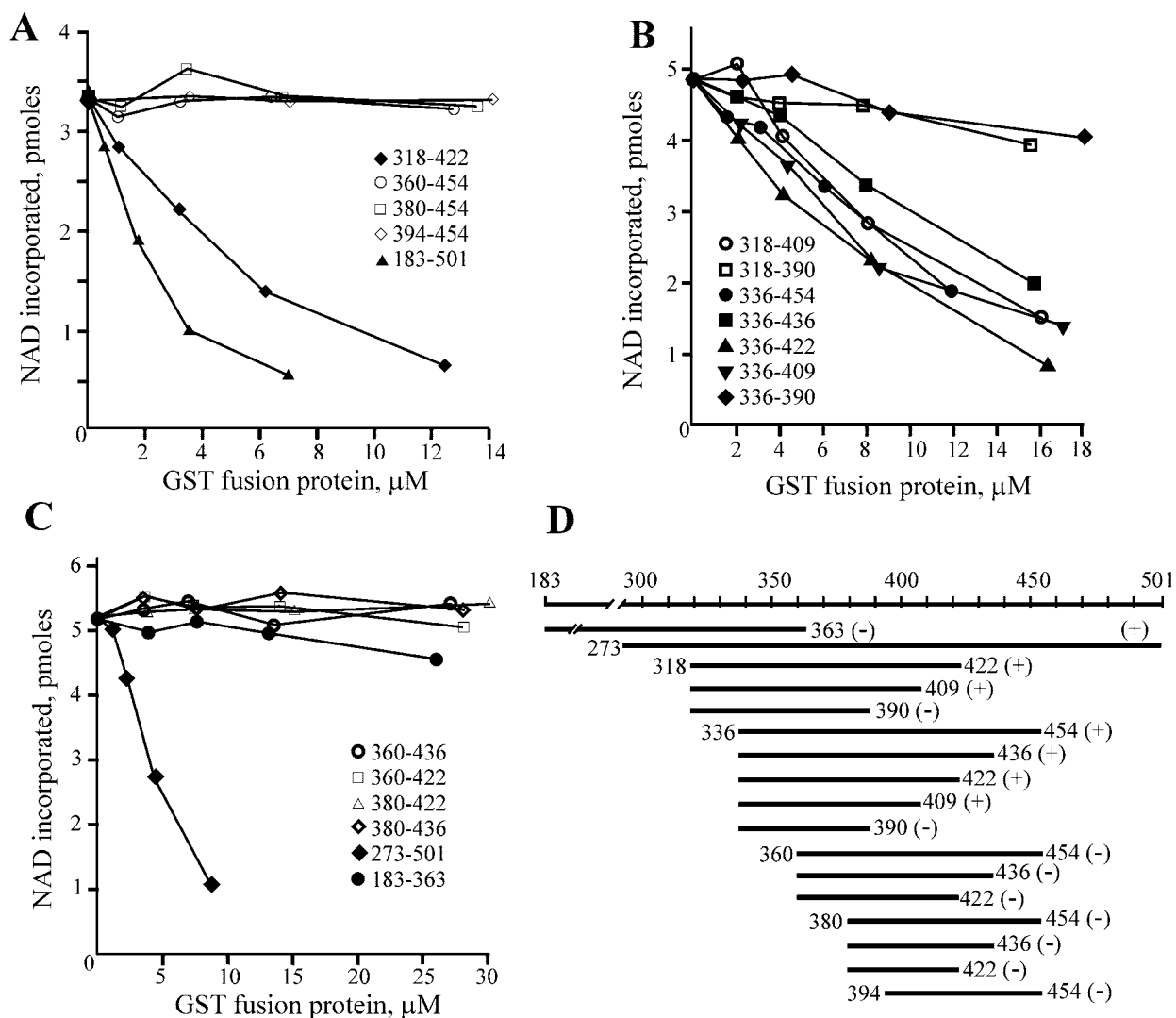


FIG. 3. Fusion proteins from the C terminus of GIRK1 inhibit G β γ -dependent, pertussis toxin-catalyzed ADP-ribosylation of G α_{i1} . A–C, results of three separate experiments in which the ability of GST-fused fragments of GIRK1 to inhibit the incorporation of NAD into purified G α_{i1} was monitored. Each experimental point is an average of a duplicate measurement and is representative of at least two independent experiments. D, schematic representation of the GST fusion proteins used in this assay and the summary of results is shown.

the depletion of intracellular Na⁺ in the low-Na⁺ external solution (26). As reported previously for GIRK1/4 channels (19), the mutations of either N-terminal histidine or the proximal C-terminal leucine greatly reduced both I_{basal} and the ACh-evoked current (I_{ACh}) (Fig. 4B, a). The basal and the evoked currents were reduced by about the same extent, as evident from the unchanged ratio R_a ($I_{\text{ACh}}/I_{\text{basal}}$; see Ref. 23) (Fig. 4B, b). This is in line with a general impairment of GIRK gating. The channels with mutated distal Leu (GIRK1_{L333E}/GIRK2_{L344E}) also showed a greatly reduced I_{basal} (Fig. 4A; note the difference in vertical calibration in the right and left panels; summarized in Fig. 4B). The average reduction of I_{basal} was close to 88% ($p < 0.01$), which is at odds with the data obtained with homomeric GIRK4 or heterotetrameric GIRK1/4, where I_{basal} was almost unaffected by this mutation (18). On the other hand, like in GIRK1/4, the agonist-evoked current was reduced even more than I_{basal} , by 98.2%, and R_a was significantly decreased compared with WT GIRK1/2 ($p < 0.05$).

To examine whether the unexpected reduction in I_{basal} in GIRK1_{L333E}/GIRK2_{K344E} is due to a change in the amount of channel protein in the plasma membrane, we have expressed WT and mutant channels at 1 ng of RNA per oocyte, to ensure high level of expression (23). Fig. 5A shows that at this expression level, I_{basal} of the mutant channel was reduced by 92%,

and I_{ACh} was reduced by 97%, compared with the WT channel. R_a of the mutant was significantly lower than in WT (Fig. 5A). The level of GIRK protein in the plasma membrane was studied by confocal imaging of antibody-stained channels in large membrane patches attached to coverslips (23). Robust expression of the GIRK1_{L333E}/GIRK2_{L344E} mutant was clearly seen, but it appeared lower than that of the WT channel (Fig. 5B). Quantitative analysis showed that the surface expression of the mutant expressed was 52% lower than of WT GIRK1/2 ($p < 0.05$; Fig. 5C). This, however, cannot explain the ~90% smaller I_{basal} in the mutant as compared with WT. The basal currents in mutant channels in the experiments of Figs. 4 and 5, corrected for the differences in expression levels, are still 73–85% smaller than in WT.

To explore further the nature of the basal activity in this mutant, we have coexpressed a general G β γ scavenger, m-c β ARK (the C-terminal part of the β -adrenergic receptor kinase 1 that carries a myristoylation signal to ensure membrane targeting of the protein) (23, 38). The effect of m-c β ARK is shown in Fig. 5D. Here basal and ACh-evoked GIRK currents in the m-c β ARK-treated groups of oocytes are shown as percentage of currents in the corresponding untreated group. Both in WT and in the mutant channel, m-c β ARK almost completely eliminated I_{ACh} , suggesting high efficiency of G β γ scavenging.

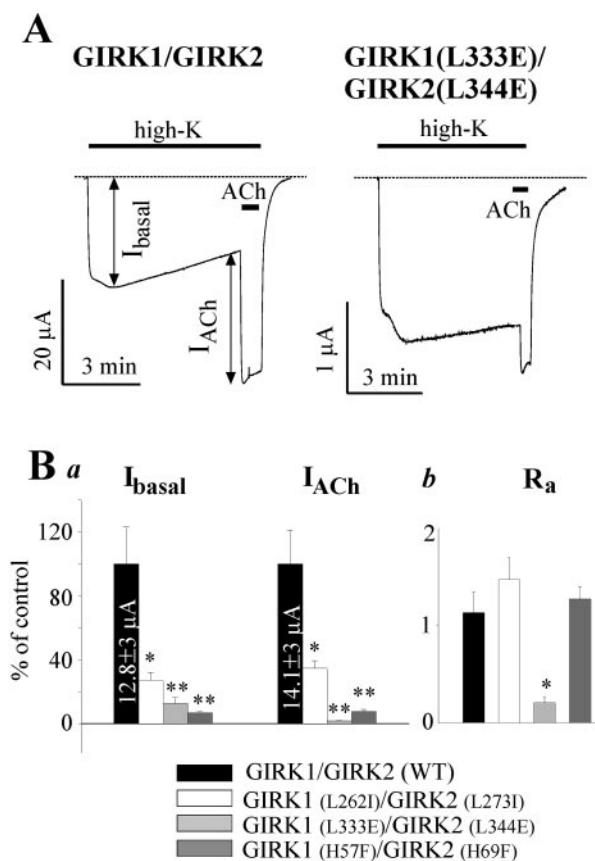


FIG. 4. The effects of mutations on whole-cell currents via heterotetrameric GIRK1/2 channels expressed in *Xenopus* oocytes. *A*, typical GIRK1/2 currents in oocytes injected with 1 ng of RNA of each channel subunit and 0.5 ng of RNA of m2R. *B*, comparison of the effects of various mutations of currents via GIRK1/2 channels (a) and on R_a (b) in oocytes of one donor, 4–5 oocytes in each group. In *a*, all currents were normalized to the control (WT) group. *, $p < 0.05$; **, $p < 0.01$ by one-way analysis of variance.

However, both in WT and the mutant channel, substantial basal activity remained, suggesting the presence of a certain G $\beta\gamma$ -independent component in I_{basal} . This component was greater in GIRK1_{L333E}/GIRK2_{L344E} ($65.6 \pm 8.6\%$) than in WT ($36.3 \pm 3\%$, $p < 0.05$).

The reduction in both evoked and basal activity in the GIRK1_{L333E}/GIRK2_{L344E} mutant indicates a general defect in G $\beta\gamma$ sensitivity (not only to agonist-released but also to “basal” G $\beta\gamma$), or a defect in G $\beta\gamma$ -dependent gating, in this mutant. The mutation of the corresponding leucine in the GST-fused C terminus of GIRK4 has been reported to cause a ~60% reduction in the binding of G $\beta\gamma$ (18). We have examined the effect of this mutation on binding of *in vitro* synthesized G $\beta\gamma$ to GST fusion fragments of the C terminus of GIRK1 and GIRK2. After correction for the amount of loaded fusion protein (Fig. 6A, upper panel), it appeared that the L333E mutation caused a 30–40% reduction in the amount of G $\beta\gamma$ bound to the full-length C terminus of GIRK1, G1-(183–501), compared with WT G1-(183–501) (Fig. 6A, lower panel). However, no reduction of G $\beta\gamma$ binding to the G1-C3 GST fusion protein could be detected after L333E mutation (Fig. 6B), even after correction for loaded protein (data not shown). We also did not observe any difference in G $\beta\gamma$ binding in the G1-C2 fragment of GIRK1, in which Leu²⁶² was mutated to Ile (Fig. 6B). Finally, we also did not see significant differences in the binding of G $\beta\gamma$ to the G2-C2-1 fragment of GIRK2 after the mutation of Leu³⁴⁴ (Fig. 6C).

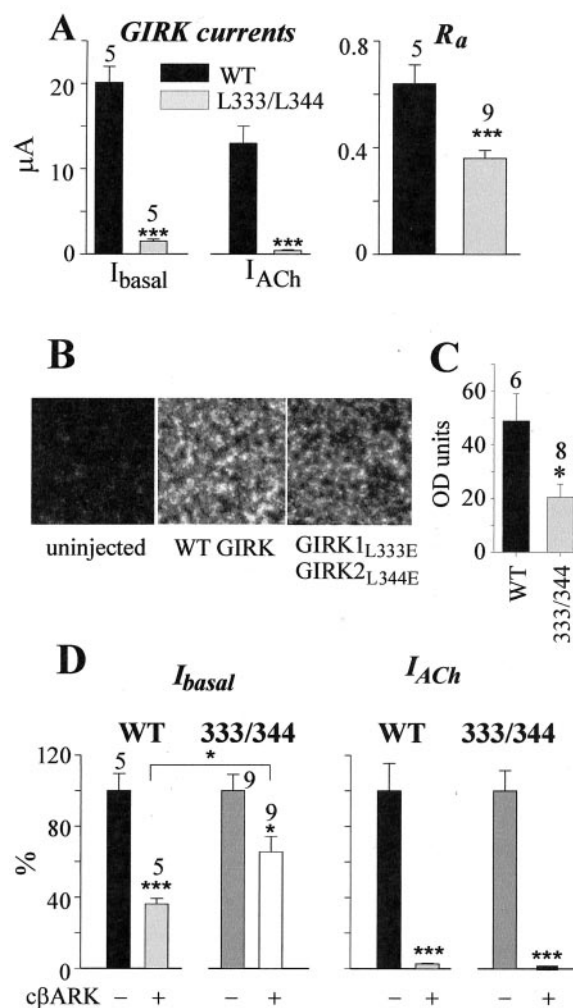


FIG. 5. The effects of GIRK1_{L333E}/GIRK2_{L344E} mutation on protein levels and whole-cell currents of heterotetrameric GIRK1/2 channels. Oocytes were injected with 1 ng of RNA of each channel subunit and 0.5 ng of RNA of m2R. Number of oocytes tested is indicated above the bars. Summary of experiments in one (WT) or two (GIRK1_{L333E}/GIRK2_{L344E}) oocyte batches is shown. *A*, whole-cell currents. In the left panel, results from oocytes from one donor only have been summarized, to allow direct comparison of current amplitudes without normalization. R_a , a dimensionless parameter, was very similar in both experiments with the GIRK1_{L333E}/GIRK2_{L344E} mutant; therefore, the results have been combined. *B*, representative confocal images of channel protein staining in large membrane patches of one oocyte batch. Image dimensions are $40 \times 40 \mu\text{m}$. Injected RNAs are indicated below the images. *C*, summary of the measurements of GIRK protein expression in the plasma membrane in oocytes of one donor. Signal intensity, in arbitrary units, was averaged after subtracting, in each image, the average intensity of signal measured in uninjected oocytes (26.4 ± 0.4 units, $n = 3$). *D*, the effect of coexpression of 5 ng of RNA of m-cBARK on GIRK currents. See explanations in the text. *, $p < 0.05$; ***, $p < 0.001$ by two-tailed *t* test.

DISCUSSION

We report the mapping of G $\beta\gamma$ -binding sites in the GIRK2 (Kir3.2) subunit of the Kir3 channels. We have also have verified and extended the map of G $\beta\gamma$ -binding sites in the GIRK1 subunit, using two independent approaches. In both subunits, the N terminus binds G $\beta\gamma$. In the C terminus, the G $\beta\gamma$ -binding sites in the two subunits are not identical; GIRK1, but not GIRK2, has a previously unrecognized G $\beta\gamma$ -interacting surface in the first half of the C terminus. The main C-terminal G $\beta\gamma$ -binding segment (a.a. 320–409 in GIRK1), found in both subunits studied, is well exposed to the outer surface of the “cytoplasmic pore” identified by Nishida and MacKinnon (12), facing the cytoplasm. Two C-terminal leucine residues, previously

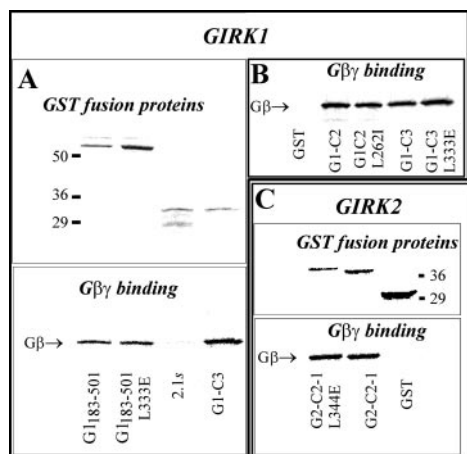


FIG. 6. Mutations of C-terminal leucines crucial for gating do not substantially affect the binding of G β γ to relevant GST-fused fragments of GIRK1 and GIRK2. Each panel shows a representative result of at least two separate determinations. *A*, binding of *in vitro* synthesized G β γ to the indicated fusion proteins of GIRK1 (lower panel). Coomassie Blue-stained proteins are shown in the upper panel. *B*, another experiment with fragments of GIRK1, with or without mutations within G2-C2 and G2-C3 fragments. *C*, binding of *in vitro* synthesized G β γ to WT or mutant G2-C2-1 fusion protein of GIRK2.

recognized as crucial for the effects of G β γ on the channel, appear to be mainly important for the regulation of G β γ -induced changes in channel gating, rather than for G β γ binding.

The G β γ -binding Segments in GIRK1 and GIRK2—Direct measurements with GST fusion proteins demonstrated G β γ binding in the distal half of the N terminus of GIRK2. This is in line with the previous reports regarding GIRK1 (13, 15, 17) and GIRK4 (19). The high conservation of the N-terminal G β γ -binding site suggests an important role for this segment in the interaction of GIRK channels with G β γ . In this work, however, we focused mainly on the interaction of G β γ with the C terminus, which makes up the bulk of the cytoplasmic domain of GIRK channel protein. To facilitate further discussion, an alignment of the C termini of GIRK1, GIRK2, and GIRK4 is shown in Fig. 7A, which also indicates some of the GST fusion segments used in this study.

The possibility of incorrect folding of protein fragments, or a fortuitous exposure to solution of a.a. residues normally buried within the native protein, is a general problem in using the fragments of a protein to map binding sites. An absence of G β γ binding to a particular fragment does not unequivocally refute its participation in G β γ binding in the native protein. Similarly, GST-fused fragments of a protein that bind G β γ may not necessarily participate in the formation of a G β γ -binding site in the native protein. These reservations call for caution in the interpretation of binding data and for the use of supportive or alternative methodologies. In GIRK1, the C-terminal G β γ -binding surface has been a subject of controversy. We used two independent methods in an attempt to refine the location of G β γ -binding site(s): a direct binding (pull-down) approach and a competition assay. In a complementary approach, we have also compared the effects of mutations of amino acids known to play crucial roles in the activation of the channel by G β γ , on G β γ binding to corresponding channel fragments, and, in parallel, on channel function and on the surface density of expressed channels.

The competition of GST-fused fragments of GIRK1 with G α for binding to G β γ was used here to chart G β γ -binding segments of GIRK. Interaction with GIRK is known to involve G β residues that participate in binding to G α (36), as well as residues outside the G α -binding surface (39–41). The competition assay is expected to reveal primarily proteins that di-

rectly compete with G α for binding to G β γ , in our case, those fragments of GIRK that interact with the G α -binding surface of G β . An allosteric effect, in which the binding of a fusion protein to a different surface of G β (or to G γ) reduces interaction of G β γ with G α , cannot be ruled out but appears less likely. Within the C terminus of GIRK1, this method revealed a G β γ -binding segment between a.a. residues 336 and 409. This segment partly overlaps G1-C3 but extends well beyond the latter, into G1-C4 (a.a. 362–411) which, by itself, did not bind G β γ in a direct assay.

Direct binding experiments with fragments of GIRK1 implicated the C terminus as composed of several independent G β γ -binding segments. G β γ bound to a large fragment, a.a. 183–363, and to separate non-overlapping subdivisions encompassing a.a. 181–254 (G1-C1), 254–319 (G1-C2), and 320–370 (G1-C3). Strong binding of G β γ to G1-C1 and G2-C2 is surprising, because these segments of GIRK have not been designated as G β γ -binding sites in GIRK1. However, the result itself does not contradict previous publications, which reported moderate (17) or strong (15) binding of G β γ to fusion proteins of a.a. 180–374 and 182–357, respectively; shorter fusion proteins corresponding to G1-C1 or G1-C2 have not been tested in the past. We sought to support the role of C1-G2 by mutating Leu²⁶², which is located in G1-C2 and is important for activation of the channel by G β γ . It has been reported that G β γ binding is reduced by mutation of a homologous Leu to Ile in the C terminus of GIRK4 (19). However, in GIRK1, the mutation Leu²⁶² → Ile did not significantly alter the binding of G β γ to the G1-C2 fragment. Therefore, if Leu²⁶² is a part of a unique G β γ -binding site in GIRK1, its contribution to the binding does not appear to be critical. In GIRK2, neither G2-C1 (a.a. 194–310) nor G2-C1-2 (a.a. 250–320; includes the corresponding Leu²⁷³) bound G β γ . The strong reduction of basal and agonist-induced currents in the heterotetrameric GIRK1/2 channels (Fig. 4) by the mutation of these homologous leucines may thus be due to a general effect on gating, rather than on G β γ binding. In all, although the direct binding experiments suggest a role for the proximal part of GIRK1 (a.a. 183–310) in the formation of G β γ -binding surface in GIRK1, such a role cannot yet be definitely assigned, awaiting additional supportive evidence obtained by an independent method.

A major role in G β γ binding in GIRK1 and GIRK2 can be definitely assigned to the segment roughly corresponding to G1-C3 but exceeding the latter in GIRK1. This is supported by two lines of evidence. 1) Both in GIRK1 and GIRK2, this segment binds G β γ in a direct assay. 2) As detected by the competition assay in GIRK1, it contains crucial binding determinants. The boundaries of this G β γ -binding segment estimated by the two methods are somewhat different, but overall it appears to extend approximately between a.a. residues 320 and 409 in GIRK1, overlapping the previously identified site 3 and part of site 4 (see Introduction and Fig. 1A). Within this G β γ -binding area in GIRK1, a.a. 336–360 and 390–409 are necessary, although insufficient, to ensure a successful competition between GIRK1 and G α for the binding to G β γ . The inability of these small fragments to bind G β γ implies an improper folding and/or lack of a definite short, high affinity G β γ -binding motif. This may explain the failure of 20-a.a.-long peptides, derived from this part of GIRK1, to prevent binding of G β γ to purified GIRK1/4 channels (20). Thus, the folding of the whole surface appears crucial for G β γ binding.

The Role of C-terminal Leucines in Basal and Agonist-evoked Activity—The identified C-terminal G β γ -binding surface includes Leu³³³ in GIRK1 and the corresponding Leu³⁴⁴ in GIRK2. Mutation of these residues to glutamate in GIRK1/4 dramatically altered channel function (18). Similarly, the

spare a larger portion of I_{basal} in the mutant. Further study will be necessary to find out whether a G β γ -independent component of I_{basal} actually exists. It is also important to note that mechanisms of basal activity may be different in GIRK1/2 and in GIRK1/4 channels. The latter usually has a lower basal activity and a higher R_a than GIRK1/2 when expressed in oocytes in similar amounts.⁴ Further study of such subtle differences between GIRK2 and GIRK4 may provide clues to residues crucial for the control of basal and agonist-evoked activity.

G β γ -binding Surface and the Three-dimensional Structure of GIRK1—It is now possible to locate the G β γ -binding segment(s) found in GIRK1 within the three-dimensional structure of GIRK1 (12). The main identified G β γ -binding surface (a.a. 320–409) is perfectly positioned to bind protein partners (Fig. 7B, *white coloring*); it constitutes the cytoplasmic part of the C terminus most exposed to the cytoplasm and partially overlaps the stretch implicated in G β γ binding on the basis of structural homology between this part of GIRK1 and the G β γ -binding surface of phosducin (12). The N-terminal G β γ -binding segment is close and probably also participates in G β γ binding. Note, however, that a distal part of the G β γ -binding surface determined here (a.a. 372–409) is missing from the available crystal structure. The parts of the C terminus corresponding to G1-C1 (*blue coloring* in Fig. 7B) and G1-C2 (*green coloring*) are much less exposed to the cytosol; large portions of these segments form the lining and the walls of the cytosolic pore. The inner vestibule of the pore is almost certainly too narrow to allow the passage of proteins, and there is little chance that G β γ can bind to residues facing it. However, certain parts of G1-C1 and G1-C2 are exposed to the cytosol and positioned close to segments of the G1-C3, identified as crucial for G β γ binding. In G1-C2, it is the loop-3₁₀ segment between a.a. 274 and 290. In G1-C1, it is the loop formed by a.a. 206–208 (conserved in GIRK1 and GIRK2 but not in GIRK4; see Fig. 7A) and the adjacent parts of two β -sheets. Importantly, this part of G1-C2 overlaps the putative G β γ -binding site 2 of GIRK4, although it has not been identified as such in GIRK1 (20). It is also notable that the primary sequence of GIRK1 between a.a. 281 and 290 is a region of low homology with GIRK2 or GIRK4, within an otherwise high homology area (see Fig. 7A). If G1-C2 indeed participates in the binding of G β γ in native GIRK1, this sequence variability might explain why the corresponding segment of GIRK2 does not bind G β γ *in vitro*. The exposed segments of G1-C1 and G1-C2 may participate in G β γ binding together with a spatially adjacent part of G1-C3. The spatial proximity of these segments within what appears to be a crucial component of the three-dimensional G β γ binding site may explain the apparent multitude of G β γ -binding fragments in GIRK1. Furthermore, it is plausible that the available crystal structure of the cytoplasmic pore corresponds to a closed channel; some of the above parts of the C terminus may become available for G β γ binding only in the open conformation.

Based on the results of the competition assay, one can speculate that all or parts of a large segment (a.a. ~336–409), spanning all the 60 Å length of the external wall of the cytosolic pore and even extending beyond, interact with the G α -binding surface of G β γ . A proximal part of G1-C3 (a.a. ~320–336), and possibly the adjacent parts of G1-C1 and G1-C2 mentioned above, may interact with other surfaces of G β γ . This would explain why neither G1-(183–363) nor G1-(318–390) (which encompass G1-C1, G1-C2 and G1-C3 but lack the segment

390–409) prevents ADP-ribosylation of G α , despite definite G β γ binding detected by the direct assay.

The contribution of different subunits to gating in a GIRK heterotetramer is asymmetrical (19, 42). Our results indicate that this is also true regarding the G β γ binding. Cross-linking experiments suggest the binding of four G β γ per purified GIRK1/4 or GIRK4 tetramer (43). Although it is tempting to assume binding of one G β γ per GIRK subunit, it remains possible that segments from two or more subunits form the actual binding sites. The relationships between the high and low affinity G β γ -binding sites (if any) in the different GIRK subunits, basal and agonist-evoked activity of GIRK, and G β γ stoichiometry have yet to be better understood.

Acknowledgments—We thank A. G. Gilman for advice and encouragement and D. E. Logothetis for providing mutants of human GIRK1 cDNA that were used in some preliminary experiments.

REFERENCES

- Clapham, D. E., and Neer, E. J. (1997) *Annu. Rev. Pharmacol. Toxicol.* **37**, 167–203
- Dascal, N. (1997) *Cell. Signal.* **9**, 551–573
- Yamada, M., Inanobe, A., and Kurachi, Y. (1998) *Pharmacol. Rev.* **50**, 723–757
- Krapivinsky, G., Gordon, E. A., Wickman, K., Velimirovic, B., Krapivinsky, L., and Clapham, D. E. (1995) *Nature* **374**, 135–141
- Lesage, F., Guillemare, E., Fink, M., Duprat, F., Heurteaux, C., Fosset, M., Romey, G., Barhanin, J., and Lazdunski, M. (1995) *J. Biol. Chem.* **270**, 28660–28667
- Inanobe, A., Ito, H., Ito, M., Hosoya, Y., and Kurachi, Y. (1995) *Biochem. Biophys. Res. Commun.* **217**, 1238–1244
- Kofuji, P., Davidson, N., and Lester, H. A. (1995) *Proc. Natl. Acad. Sci. U. S. A.* **92**, 6542–6546
- Jelacic, T. M., Sims, S. M., and Clapham, D. E. (1999) *J. Membr. Biol.* **169**, 123–129
- Bettahi, I., Marker, C. L., Roman, I. M., and Wickman, K. (2002) *J. Biol. Chem.* **277**, 48282–48288
- Jan, L. Y., and Jan, Y. N. (1997) *J. Physiol. (Lond.)* **505**, 267–282
- Doyle, D. A., Morais Cabral, J., Pfuetzner, R. A., Kuo, A., Gulbis, J. M., Cohen, S. L., Chait, B. T., and MacKinnon, R. (1998) *Science* **280**, 69–77
- Nishida, M., and MacKinnon, R. (2002) *Cell* **111**, 957–965
- Huang, C. L., Slesinger, P. A., Casey, P. J., Jan, Y. N., and Jan, L. Y. (1995) *Neuron* **15**, 1133–1143
- Krapivinsky, G., Krapivinsky, L., Wickman, K., and Clapham, D. E. (1995) *J. Biol. Chem.* **270**, 29059–29062
- Kunkel, M. T., and Peralta, E. G. (1995) *Cell* **83**, 443–449
- Doupnik, C. A., Dessauer, C. W., Slepak, V. Z., Gilman, A. G., Davidson, N., and Lester, H. A. (1996) *Neuropharmacology* **35**, 923–931
- Huang, C. L., Jan, Y. N., and Jan, L. Y. (1997) *FEBS Lett.* **405**, 291–298
- He, C., Zhang, H., Mirshahi, T., and Logothetis, D. E. (1999) *J. Biol. Chem.* **274**, 12517–12524
- He, C., Yang, X., Zhang, H., Mirshahi, T., Jin, T., Huang, A., and Logothetis, D. E. (2002) *J. Biol. Chem.* **277**, 6088–6096
- Krapivinsky, G., Kennedy, M. E., Nemeč, J., Medina, I., Krapivinsky, L., and Clapham, D. E. (1998) *J. Biol. Chem.* **273**, 16946–16952
- Wang, C. R., Esser, L., Smagula, C. S., Sudhof, T. C., and Deisenhofer, J. (1997) *Protein Sci.* **6**, 2264–2267
- Lesage, F., Duprat, F., Fink, M., Guillemare, E., Coppola, T., Lazdunski, M., and Hugnot, J. P. (1994) *FEBS Lett.* **353**, 37–42
- Peleg, S., Varon, D., Ivanina, T., Dessauer, C. W., and Dascal, N. (2002) *Neuron* **33**, 87–99
- Rishal, I., Keren-Raifman, T., Yakubovich, D., Ivanina, T., Dessauer, C. W., Slepak, V. Z., and Dascal, N. (2003) *J. Biol. Chem.* **278**, 3840–3845
- Dascal, N., Schreibmayer, W., Lim, N. F., Wang, W., Chavkin, C., DiMugno, L., Labarca, C., Kieffer, B. L., Gaveriaux-Ruff, C., Trollinger, D., Lester, H. A., and Davidson, N. (1993) *Proc. Natl. Acad. Sci. U. S. A.* **90**, 10235–10239
- Vorobiov, D., Levin, G., Lotan, I., and Dascal, N. (1998) *Pfluegers Arch.* **436**, 56–68
- Lee, E., Linder, M. E., and Gilman, A. G. (1994) *Methods Enzymol.* **237**, 146–164
- Kozasa, T., and Gilman, A. G. (1995) *J. Biol. Chem.* **270**, 1734–1741
- Shistik, E., Ivanina, T., Blumenstein, Y., and Dascal, N. (1998) *J. Biol. Chem.* **273**, 17901–17909
- Casey, P. J., Pang, I. H., and Gilman, A. G. (1991) *Methods Enzymol.* **195**, 315–321
- Ivanina, T., Perets, T., Thornhill, W. B., Levin, G., Dascal, N., and Lotan, I. (1994) *Biochemistry* **33**, 8786–8792
- Robillard, L., Ethier, N., Lachance, M., and Hebert, T. E. (2000) *Cell. Signal.* **12**, 673–682
- Singer-Lahat, D., Dascal, N., Mittelman, L., Peleg, S., and Lotan, I. (2000) *Pfluegers Arch.* **440**, 627–633
- Zamponi, G. W., Bourinet, E., Nelson, D., Nargeot, J., and Snutch, T. P. (1997) *Nature* **385**, 442–446
- Ivanina, T., Blumenstein, Y., Shistik, E., Barzilai, R., and Dascal, N. (2000) *J. Biol. Chem.* **275**, 39846–39854
- Ford, C. E., Skiba, N. P., Bae, H., Daaka, Y., Reuveny, E., Shekter, L. R., Rosal, R., Weng, G., Yang, C. S., Iyengar, R., Miller, R. J., Jan, L. Y., Lefkowitz, R. J., and Hamm, H. E. (1998) *Science* **280**, 1271–1274

⁴ N. Dascal, unpublished observations.

37. Gilman, A. G. (1987) *Annu. Rev. Biochem.* **56**, 615–649
38. Petit-Jacques, J., Sui, J. L., and Logothetis, D. E. (1999) *J. Gen. Physiol.* **114**, 673–684
39. Albsoul-Younes, A. M., Sternweis, P. M., Zhao, P., Nakata, H., Nakajima, S., Nakajima, Y., and Kozasa, T. (2001) *J. Biol. Chem.* **276**, 12712–12717
40. Mirshahi, T., Mittal, V., Zhang, H., Linder, M. E., and Logothetis, D. E. (2002) *J. Biol. Chem.* **277**, 36345–36350
41. Mirshahi, T., Robillard, L., Zhang, H., Hebert, T. E., and Logothetis, D. E. (2002) *J. Biol. Chem.* **277**, 7348–7355
42. Sadjia, R., Alagem, N., and Reuveny, E. (2002) *Proc. Natl. Acad. Sci. U. S. A.* **17**, 10783–10788
43. Corey, S., and Clapham, D. E. (2001) *J. Biol. Chem.* **276**, 11409–11413